Electronic Properties of Electron-Deficient Zn(II) porphyrins for HBr splitting

1. Synthesis of 4-(7-bromobenzo[1,2,5]thiadiazol-4-yl)benzaldehyde

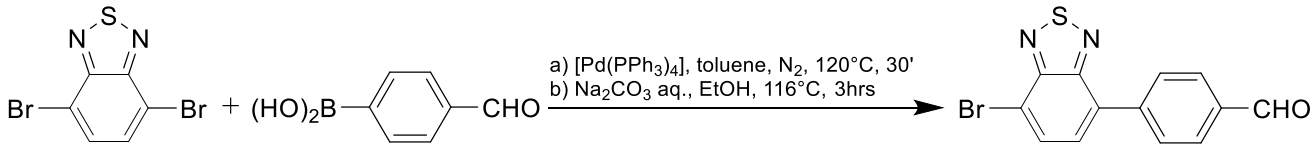

Scheme S1.

In a dry Schlenk tube, under stirring and N_2 flow, 2.7 mmol (800 mg) of 4,7-dibromobenzo[1,2,5]thiadiazole, 2.7 mmol (405 mg, 1 eq.) of (4-formylphenyl)boronic acid and 0.064 mmol (0.074 mg, 0.2 eq.) of [$Pd(PPh_3)_4$] were dissolved in toluene (40 mL). The mixture was degassed by performing 3 cycles of freeze-pump-thaw at -78 °C, and refluxed for 30 min. After this time, a 2 M Na_2CO_3 aqueous solution (4.26 g in 20 mL of H_2O) and EtOH (12 mL) (both degassed) were added in the Schlenk tube, then the whole mixture was stirred at 116°C for 3 hrs. After cooling down at RT, the crude product was extracted by washing the mixture with a saturated NaCl aqueous solution (3 × 20 mL) and extracted with CH_2Cl_2 (3 × 20 mL). The organic layer was dried over Na_2SO_4 and the solvent evaporated *in vacuo*. The crude was purified by flash chromatography (*n*-hexane:CH_2Cl_2 = 1:1), through a *Biotage Isolera One* system, using a 25 g silica plug. After evaporation of the solvents, the desired product was collected as a pale-yellow powder (322.2 mg, 37% yield).
^{1}H-NMR (400 *MHz*, $CDCl_3$, 25 °C) δ, *ppm*: 10.14 (1H, s), 8.12 (2H, d), 8.07 (2H, d), 8.00 (1H, d), 7.68 (1H, d).

2. Time Resolved Fluorescence

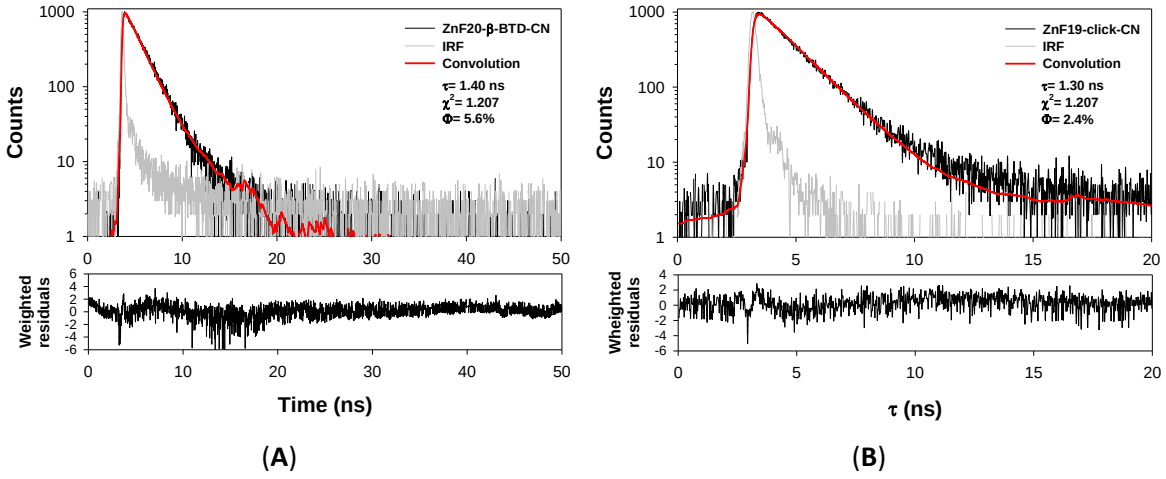

Figure S1. Fluorescence decay of porphyrin 1 (**A**) and 2 (**B**) in toluene solution, bold black line (λ_{exc} = 442 nm; λ_{em} = 642 nm). Convolution fit, red line. Weighted residuals are shown under the decay curves.

3. Electrochemical Properties in Organic Solvent

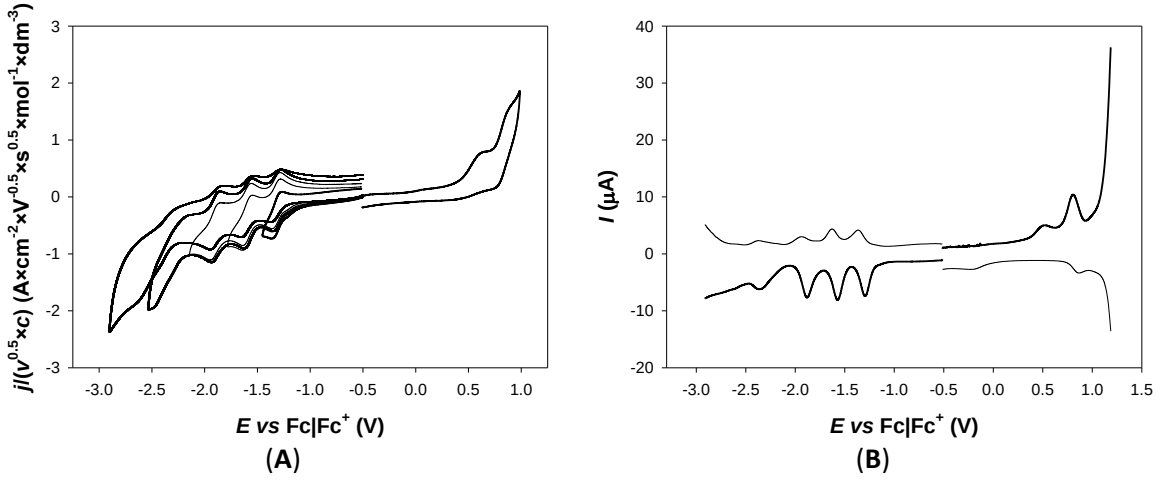

Figure S2. CV (**A**) and DPV (**B**) of porphyrin **1** on glassy carbon electrode, in DMF+0.1 M TBAP, at 0.2 V·s$^{-1.}$

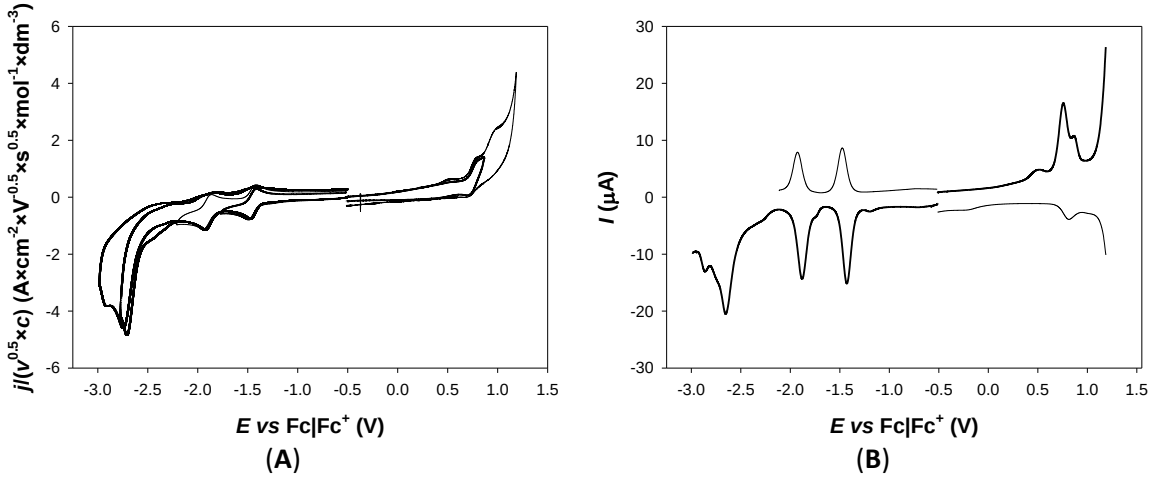

Figure S3. CV (**A**) and DPV (**B**) of porphyrin **2** on glassy carbon electrode, in DMF+0.1 M TBAP, at 0.2 V·s$^{-1.}$

Table S1. Electrochemical energy levels of porphyrins **1** and **2**, referred to the ferrocenium/ferrocene redox couple.

Dye	$E^{0'}_{Ia}$/V (Fc^+|Fc)	$E^{0'}_{Ic}$/V(Fc^+|Fc)	HOMO/eV	LUMO/eV	$\Delta E^{0'}$/V($E_{g,EC}$/eV)
1	0.83	−1.32	−5.63	−3.48	2.15
2	0.76	−1.45	−5.56	−3.35	2.21

4. Photoelectrochemistry

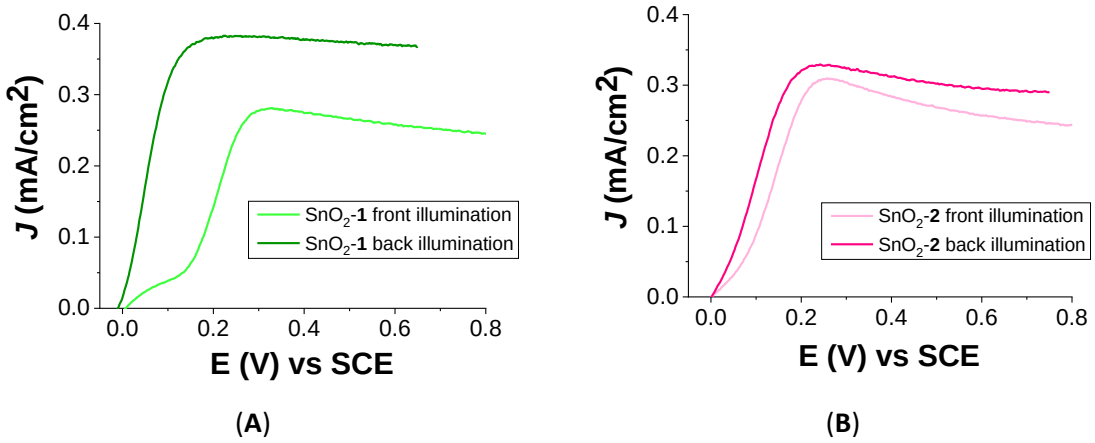

Figure S4. Net photocurrents (i.e. after the subtraction of the dark contribution) recorded for SnO_2-1 (**A**) and SnO_2-2 (**B**) photoanodes in 0.1 M HBr (pH 1) under 1 sun (0.1 mW/cm²) AM 1.5 G illumination from both the back side of the electrode (i.e. the FTO side) and the front side (i.e. from the electrolytic solution). Average curves of 5–7 electrodes are reported.

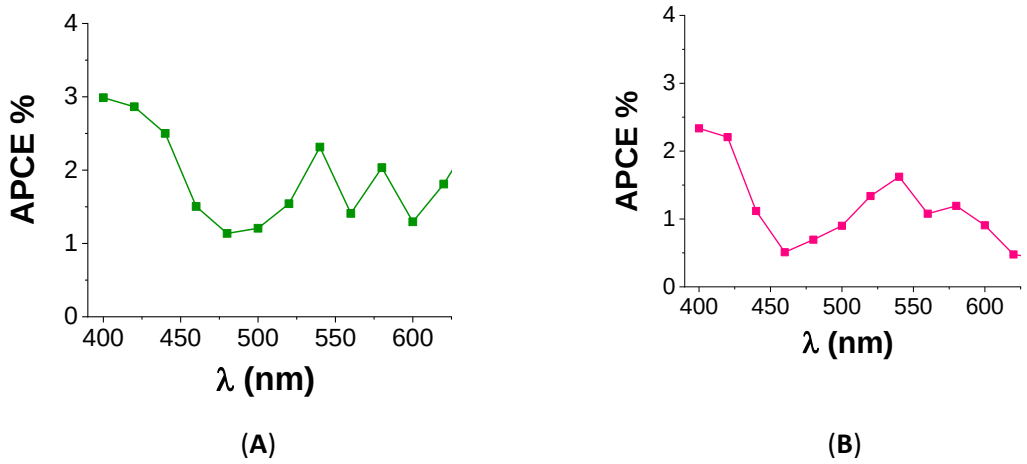

Figure S5. APCE spectra of SnO_2-**1** (**A**) and SnO_2-**2** (**B**) photoanodes recorded in 0.1 M HBr (pH 1) under 0.6 V vs SCE applied bias. Illumination was through the FTO.

5. Time Resolved Absorption Spectroscopy

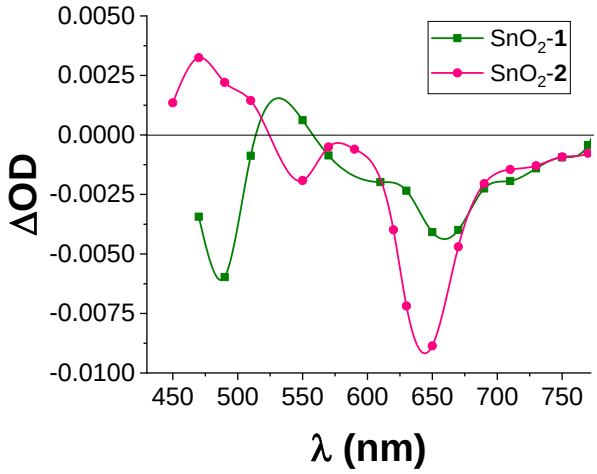

Figure S6. Transient spectra of SnO_2-**1** (A) and SnO_2-**2** (B) photoanodes at OCP in 0.1 M $HClO_4$ as an inert electrolyte taken at 0 delay. Notice the apparent bleaching in the 600–750 region, due to spontaneous emission.

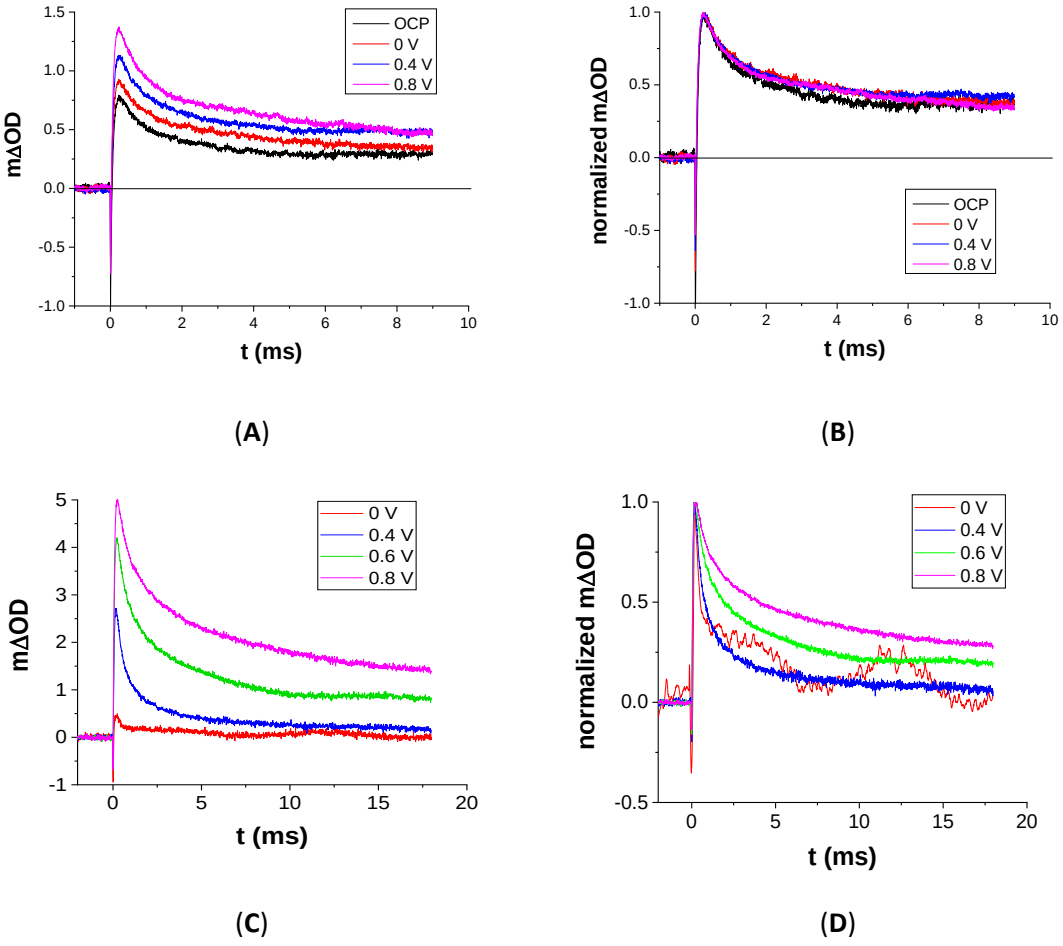

Figure S7. Kinetic evolution of $SnO_2(e^-)$-**1**(h^+) (**A**–**B**) and $SnO_2(e^-)$-**2**(h^+) (**C**–**D**) charge separated states after the ns laser excitation at 532 nm in 0.1 M HBr + 0.3 M NaBr at OCP and under different applied biases (values vs Pt). 1 MΩ oscilloscope resistance. In (**B**) and (**D**) the traces have been normalized to unity.